Journal of the Brazilian Society of Mechanical Sciences and Engineering (2019) 41:239
https://doi.org/10.1007/s40430-019-1732-9

TECHNICAL PAPER

Size-dependent nonlinear forced oscillation of self-assembled nanotubules based on the nonlocal strain gradient beam model

S. Sahmani[1] · A. M. Fattahi[2] · N. A. Ahmed[2]

Received: 1 May 2018 / Accepted: 14 April 2019 / Published online: 27 April 2019

Abstract
Self-assembled protein micro/nanotubule has been aroused considerable interest as a self-assembled supramolecular structure with bioactive properties. The prime aim of this study is to predict size dependency in the nonlinear forced oscillation of the self-assembled nanotubules embedded in an elastic biomedium. To accomplish this end, the nonlocal strain gradient elasticity theory including both softening and stiffening features of size effect is applied to the refined hyperbolic shear deformable beam model. By using the principle of Hamilton, unconventional governing differential equations of motion have been extracted. Subsequently, generalized differential quadrature method in conjunction with the Galerkin technique is employed to solve the nonclassical problem numerically. The nonlocal strain gradient frequency response and amplitude response relevant to the primary resonance of the self-assembled nanotubules are obtained corresponding to different types of boundary conditions. It is anticipated that the nonlocal size effect causes to decrease the excitation amplitudes associated with both bifurcation points, but its effect on the first one is more considerable. However, the strain gradient size dependency has an opposite influence and leads to increase them. Furthermore, it is found that by changing the end supports from simply supported to clamped one, the influence of the nonlocality on the excitation amplitude associated with the bifurcation points increases, but the influence of the strain gradient size dependency decreases.

Keywords Nanotechnology · Biomechanics · Size dependency · Nonlinear vibrations · Nonlocal strain gradient elasticity theory

1 Introduction

In a living cell, protein micro/nanotubules as an essential cytoskeletal component play an important role in making the cell shape and its mechanical characteristics. In other words, the protein micro/nanotubules are the most rigid of the cytoskeletal biopolymers, the bending stiffness of which is about hundred times greater than that of actin filaments. Zheng et al. [1] reported that through application of tension to sensory neurons creates new microtubule assembly concomitant. Omelchanko et al. [2] concluded that microtubules provide the necessary framework for polarization of fibroblasts and epitheliocytes. Gupton et al. [3] anticipated that drugs affect the rate of F-actin and microtubule convergence as well as microtubule buckling in a central cell region.

The structure of a living cell and its components may vibrate in various frequency ranges which causes to transfer mass, signals and energy between cells. Pokorny et al. [4] indicated that deterministic forces of biological polar molecules have the capability to transport particles and electrons with higher probability than forces of thermal origin only. They also analyzed vibration states in cells using numerical models. They found that the interaction forces between cancer cells may be lower than those between healthy cells [5]. Atanasov et al. [6] developed a physical model for vibration behavior of microtubules in living cell corresponding to the first four vibration modes relevant to transverse and longitudinal waves.

Technical Editor: Paulo de Tarso Rocha de Mendonça, Ph.D.

✉ S. Sahmani
ssahmani@nri.ac.ir

✉ A. M. Fattahi
afattahi@uj.ac.za

[1] Mechanical Rotating Equipment Department, Niroo Research Institute (NRI), Tehran 14665-517, Iran

[2] Mechanical Engineering Science Department, Faculty of Engineering and Built Environment, University of Johannesburg, Johannesburg 2006, South Africa

Due to the micron and submicron size of the microtubule dimensions, small-scale effects have significant influence on its mechanical behavior. In order to take these size effects into consideration, several unconventional continuum theories of elasticity have proposed and employed to predict size-dependent mechanical responses of micro/nanostructures [7–50]. For instance, Gao and An [51] explored the buckling behavior of protein microtubules on the basis of a nonlocal anisotropic elastic shell model. Taj and Zhang [52] investigated the free vibration response of microtubules embedded in an elastic medium. Baninajjaryan and Tadi Beni [53] developed a size-dependent isotropic shell model based on the nonlocal elasticity theory for free vibration analysis of microtubules. Civalek and Demir [54] proposed a nonlocal finite element method for mechanical characteristics of protein microtubules. Tadi Beni et al. [55] predicted the size-dependent buckling behavior of protein microtubule under axial and radial compressions based on the couple stress theory of elasticity. Sahmani and Aghdam [56, 57] predicted the size-dependent nonlinear axial and radial instabilities of protein micro/nanotubules embedded in the cytoplasm of a living cell. They also anticipated the size-dependent nonlinear vibrations of axially loaded lipid protein micro/nanotubules within the prebuckling and postbuckling domains [58].

In accordance with reviewing the historical background, it is common that size effect in type of the stress nonlocality demonstrates softening influence caused a reduction in the stiffness, while the strain gradient small-scale effect plays a hardening role made an increment in the value of stiffness. It means that the previously proposed unconventional continuum theories have not the capability to cover the size dependencies in a perfect way. As a consequence, a new size-dependent theory of elasticity, namely as nonlocal strain gradient theory, was developed by Lim et al. [59] including simultaneously both softening and stiffening features of size effects. Thereafter, several investigations have been carried out using the newly proposed nonclassical continuum theory of elasticity. For instance, Li and Hu [60] employed the nonlocal strain gradient theory of elasticity to analyze the nonlinear buckling characteristics of Euler–Bernoulli nanobeams. Additionally, they predicted the nonlocal strain gradient frequency of wave motion on nanotubes conveying fluid [61]. Yang et al. [62] anticipated the critical nonlocal strain gradient voltages associated with the pull-in instability of functionally graded nanoactuators. Simsek [63] constructed a nonlocal strain gradient beam model for nonlinear vibrations of functionally graded Euler–Bernoulli nanobeams. Farajpour et al. [64] examined buckling behavior of orthotropic nonlocal strain gradient plates using a new size-dependent plate model. Tang et al. [65] analyzed the nonlocal strain gradient wave propagation in a viscoelastic nanotube. With the aid of the strain gradient elasticity theory, Sahmani and Aghdam [66] studied the linear and nonlinear vibrations of supramolecular lipid micro/nanotubules within both prebuckling and postbuckling domains. Li et al. [67] anticipated the size-dependent bending, buckling and free vibration characteristics of axially functionally graded nonlocal strain gradient beams. Lu et al. [68] explored the influences of nonlocality and strain gradient size dependency on the free vibration behavior of beams at nanoscale. Sahmani and Aghdam [69, 70] reported analytical expressions for the nonlocal strain gradient nonlinear buckling and postbuckling behavior of hydrostatic pressurized multilayer functionally graded nanoshells. Wang et al. [44] introduced a nonlocal strain gradient beam model for complex modal analysis for vibrational response of axially moving beams at nanoscale. Sahmani et al. [71–73] developed nonlocal strain gradient beam and plate models to analyze size-dependent nonlinear mechanical behaviors of functionally graded porous micro/nanostructures. Zhen et al. [74] employed the local adaptive differential quadrature method and the nonlocal strain gradient free vibrations of viscoelastic nanotubes.

In the present work, for the first time, the size-dependent nonlinear primary resonance of the protein micro/nanotubules under soft harmonic excitation and embedded in an elastic biomedium is investigated. To accomplish this purpose, the nonlocal strain gradient elasticity theory is employed within the framework of the refined hyperbolic shear deformable beam model. Via the Hamilton's principle, the nonclassical governing differential equations of motion are constructed. After that, a numerical solution methodology based upon the generalized differential quadrature (GDQ) method in conjunction with the Galerkin technique is utilized to solve the nonlinear problem.

2 Mathematical formulations

As depicted in Fig. 1, a protein micro/nanotubule created by twisting of bilayer stripe protein molecules is considered. Due to the chirality, the protein molecules cannot pack parallel of themselves. The lipid micro/nanotubule is modeled as a beam-type structure with length L, thickness h and mid-radius R. Also, a coordinate system is attached to the lipid micro/nanotubule in such a way that its z-axis is along tubule thickness and its x-axis is along tubule length.

Based upon the hyperbolic shear deformation beam theory [75], the displacement field along different coordinate directions can be written as

$$u_x(x,z,t) = u(x,t) - zw_{,x}(x,t) + \left[z\cosh(1/2) - h\sinh(z/h)\right]\psi(x,t) \tag{1a}$$

$$u_z(x,z,t) = w(x,t) \tag{1b}$$

where u and w in order are the displacement components of the biological lipid tubule along x- and z-axis. Additionally,

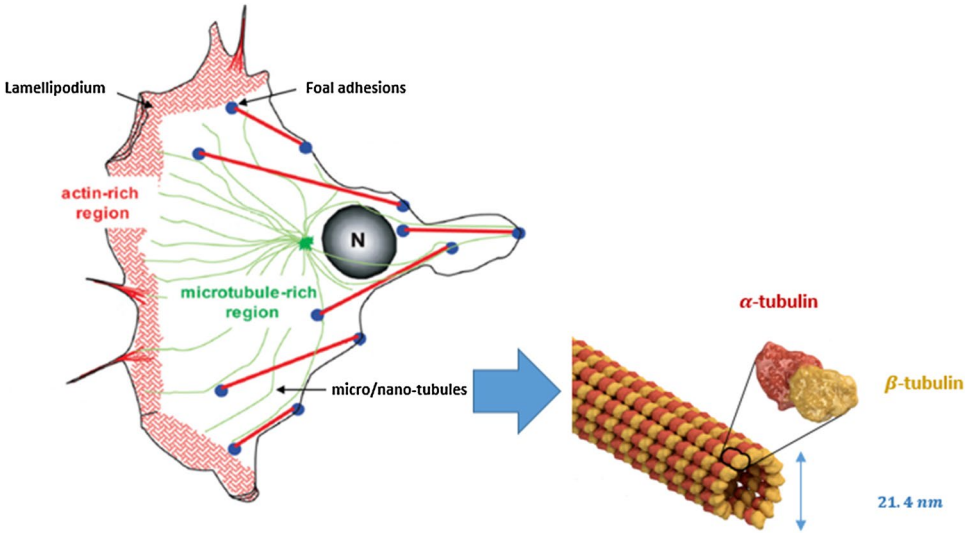

Fig. 1 Schematic view of the a living cell including protein micro/nanotubules

ψ represents the rotation with respect to the cross section of the micro/nanotubule at neutral plane normal about y-axis.

Consequently, the nonzero strain components are derived as

$$\begin{Bmatrix} \varepsilon_{xx} \\ \gamma_{xz} \end{Bmatrix} = \begin{Bmatrix} u_{,x} + (1/2)w_{,x}^2 - zw_{,xx} + \left[z\cosh(1/2) - h\sinh(z/h)\right]\psi_{,x} \\ \left[\cosh(1/2) - \cosh(z/h)\right]\psi \end{Bmatrix}$$

in which ε_{xx} and γ_{xz} denote, respectively, the normal and shear strains.

As it has been reported previously, the nonlocal elasticity theory and strain gradient elasticity theory do not consider size effect comprehensively. The nonlocal theory cannot take the higher-order stresses into account. On the other hand, the strain gradient theory has the capability to consider only local higher-order strain gradients. Motivated by this fact, Lim et al. [59] proposed a combination of these theories, namely as nonlocal strain gradient elasticity theory, which assess small-scale effects more reasonably. Accordingly, the total nonlocal strain gradient stress tensor Λ for a beam-type structure can be defined as below [59]

$$\Lambda_{xx} = \sigma_{xx} - \sigma^*_{xx,x} \tag{3a}$$

$$\Lambda_{xz} = \sigma_{xz} - \sigma^*_{xz,x} \tag{3b}$$

where σ and σ^* are the stress and higher-order stress tensors, respectively, which can be expressed as

$$\sigma_{ij} = \int_{\Omega} \left\{\varrho_1\left(\left|\mathcal{X}' - \mathcal{X}\right|\right) C_{ijkl}\varepsilon_{kl}\left(\mathcal{X}'\right)\right\} \mathrm{d}\Omega \tag{4a}$$

$$\sigma^*_{ij} = l^2 \int_{\Omega} \left\{\varrho_2\left(\left|\mathcal{X}' - \mathcal{X}\right|\right) C_{ijkl}\varepsilon_{kl,x}\left(\mathcal{X}'\right)\right\} \mathrm{d}\Omega \tag{4b}$$

in which C denotes the elastic matrix, ϱ_1 and ϱ_2 in order represent the principal attenuation kernel function in the presence of the nonlocality and the additional kernel function related to the nonlocality effect of the first-order strain gradient field, $\mathcal{X}$ and $\mathcal{X}'$ are, respectively, a point and any point else in the body, and l is the internal strain gradient length scale parameter. In accordance with the method of Eringen and assuming $\varrho_1 = \varrho_2 = \varrho$, the constitutive equation relevant to the total nonlocal strain gradient stress tensor of a beam-type structure is constructed as

$$\Lambda_{xx} - \mu^2\Lambda_{xx,xx} = C_{xxxx}\varepsilon_{xx} - l^2 C_{xxxx}\varepsilon_{xx,xx} \tag{5a}$$

$$\Lambda_{xz} - \mu^2\Lambda_{xz,xx} = C_{xzxz}\varepsilon_{xz} - l^2 C_{xzxz}\varepsilon_{xz,xx} \tag{5b}$$

where μ is the nonlocal parameter. Thereafter, the nonlocal strain gradient constitutive relations for a hyperbolic shear deformable micro/nanobeam made of nanoporous biomaterial can be expressed as

$$\begin{aligned} \Lambda_{xx} - \mu^2\Lambda_{xx,xx} &= \left[E/\left(1-\nu^2\right)\right]\Big\{u_{,x} + (1/2)\left(w_{,x}\right)^2 - zw_{,xx} + \left[z\cosh(1/2) - h\sinh(z/h)\right]\psi_{,x} \\ &\quad - l^2\left(u_{,xxx} + w_{,xxx}w_{,x} + w_{,xx}^2 - zw_{,xxxx} + \left[z\cosh(1/2) - h\sinh(z/h)\right]\psi_{,xxx}\right)\Big\} \\ \Lambda_{xz} - \mu^2\Lambda_{xz,xx} &= \left[E/2(1+\nu)\right]\left\{\left[\cosh(1/2) - \cosh(z/h)\right]\psi - l^2\left[\cosh(1/2) - \cosh(z/h)\right]\psi_{,xx}\right\} \end{aligned} \tag{6}$$

Therefore, within the framework of the nonlocal strain gradient hyperbolic shear deformable beam model, the total strain energy of a biological lipid protein micro/nanotubule can be written as

$$\begin{aligned}\Pi_s &= \frac{1}{2}\int_0^L\int_S \left\{\sigma_{ij}\varepsilon_{ij} + \sigma_{ij}^*\nabla\varepsilon_{ij}\right\}\mathrm{d}S\mathrm{d}x \\ &= \frac{1}{2}\int_0^L \left\{N_{xx}\varepsilon_{xx}^0 + M_{xx}\kappa_{xx}^{(0)} + R_{xx}\kappa_{xx}^{(2)} + Q_x\psi\right\}\mathrm{d}x\end{aligned} \tag{7}$$

in which the stress resultants can be introduced as below

$$\begin{aligned}N_{xx} - \mu^2 N_{xx,xx} &= A_{11}^*\left[u_{,x} + (1/2)w_{,x}^2 - l^2\left(u_{,xxx} + w_{,x}w_{,xxx} + w_{,xx}^2\right)\right] \\ M_{xx} - \mu^2 M_{xx,xx} &= D_{11}^*\left(-w_{,xx} + l^2 w_{,xxxx}\right) + F_{11}^*\left(\psi_{,x} - l^2\psi_{,xxx}\right) \\ R_{xx} - \mu^2 R_{xx,xx} &= F_{11}^*\left(-w_{,xx} + l^2 w_{,xxxx}\right) + H_{11}^*\left(\psi_{,x} - l^2\psi_{,xxx}\right) \\ Q_x - \mu^2 Q_{x,xx} &= A_{44}^*\left(\psi - l^2\psi_{,xx}\right)\end{aligned} \tag{8}$$

where

$$\begin{aligned}\left\{N_{xx}, M_{xx}, R_{xx}\right\} &= 2\pi R\int_{-\frac{h}{2}}^{\frac{h}{2}} \Lambda_{xx}\{1, z, z\cosh(1/2) - h\sinh(z/h)\}\mathrm{d}z \\ Q_x &= 2\pi R\int_{-\frac{h}{2}}^{\frac{h}{2}} \Lambda_{xz}\{\cosh(1/2) - \cosh(z/h)\}\mathrm{d}z\end{aligned} \tag{9}$$

and

$$\begin{aligned}\left\{A_{11}^*, D_{11}^*\right\} &= \left[2\pi RE/\left(1-\nu^2\right)\right]\int_{-\frac{h}{2}}^{\frac{h}{2}}\left\{1, z^2\right\}\mathrm{d}z \\ \left\{F_{11}^*, H_{11}^*\right\} &= \left[2\pi RE/\left(1-\nu^2\right)\right]\int_{-\frac{h}{2}}^{\frac{h}{2}}\left\{z^2\cosh(1/2) - zh\sinh(z/h),\right. \\ &\qquad \left.(z\cosh(1/2) - h\sinh(z/h))^2\right\}\mathrm{d}z \\ \left\{A_{44}^*\right\} &= \left[2\pi RE/2(1+\nu)\right]\int_{-\frac{h}{2}}^{\frac{h}{2}}\{\cosh(1/2) - \cosh(z/h)\}\mathrm{d}z\end{aligned} \tag{10}$$

Additionally, the kinetic energy for a biological lipid protein micro/nanotubule on the basis of the nonlocal strain gradient hyperbolic shear deformable beam model can be expressed as

$$\begin{aligned}\Pi_T &= \frac{1}{2}\int_0^L\int_S \rho\left\{\left(u_{x,t}\right)^2 + \left(u_{z,t}\right)^2\right\}\mathrm{d}S\mathrm{d}x \\ &= \frac{1}{2}\int_0^L \left\{I_0\left(u_{,t}\right)^2 + I_2\left(w_{,xt}\right)^2 + I_3 w_{,xt}\psi_{,t} + I_4\left(\psi_{,t}\right)^2 + I_0\left(w_{,t}\right)^2\right\}\mathrm{d}x\end{aligned}$$

where

$$\begin{aligned}&\{I_0, I_2, I_3, I_4\} \\ &= 2\pi R\rho\int_{-\frac{h}{2}}^{\frac{h}{2}}\left\{1, z^2, z^2\cosh(1/2) - zh\sinh(z/h), (z\cosh(1/2) - h\sinh(z/h))^2\right\}\mathrm{d}z\end{aligned} \tag{11}$$

The external work performed by the elastic biomedium can be written as

$$\Pi_P = \int_0^L \left(k_1 w^2 + k_2 w_{,x}^2\right)\mathrm{d}x \tag{12}$$

in which k_1 and k_2 represent the normal and shear stiffness of the elastic biomedium, respectively.

Moreover, the performed work associated with the external transverse force q can be defined as below

$$\Pi_w = \int_0^L q(x,t)w\mathrm{d}x \tag{13}$$

Afterward, based upon the Hamilton's principle, the governing differential equations of motion in terms of stress resultants are derived as

$$N_{xx,x} = I_0 u_{,tt} \tag{14a}$$

$$M_{xx,xx} + \left(N_{xx}w_{,x}\right)_{,x} - k_1 w + k_2 w_{,xx} + q = I_0 w_{,tt} - I_2 w_{,xxtt} - I_3\psi_{,xtt} \tag{14b}$$

$$R_{xx,x} - Q_x = I_3 w_{,xtt} + I_4\psi_{,tt} \tag{14c}$$

Consequently, through inserting Eq. (8) in Eq. (14), the size-dependent equations of motion can be rewritten as

$$\begin{aligned}&A_{11}^*\left[u_{,xx} + w_{,x}w_{,xx} - l^2\left(u_{,xxxx} + 3w_{,xx}w_{,xxx} + w_{,x}w_{,xxxx}\right)\right] \\ &\quad = I_0\left(u_{,tt} - \mu^2 u_{,xxtt}\right)\end{aligned} \tag{15a}$$

$$\begin{aligned}&D_{11}^*\left(-w_{,xxxx} + l^2 w_{,xxxxxx}\right) + F_{11}^*\left(\psi_{,xxx} - l^2\psi_{,xxxxx}\right) \\ &\quad + A_{11}^*\Gamma_1 - l^2 A_{11}^*\Gamma_2 - \mu^2 A_{11}^*\Gamma_3 + \mu^2 l^2 A_{11}^*\Gamma_4 \\ &= I_0\left(w_{,tt} - \mu^2 w_{,xxtt}\right) - I_2\left(w_{,xxtt} - \mu^2 w_{,xxxxtt}\right) \\ &\quad - I_3\left(\psi_{,xtt} - \mu^2\psi_{,xxxtt}\right) - q + \mu^2 q_{,xx} + k_1\left(w - \mu^2 w_{,xx}\right) \\ &\quad - k_2\left(w_{,xx} - \mu^2 w_{,xxxx}\right)\end{aligned} \tag{15b}$$

$$\begin{aligned}&\left(F_{11}^{*}\left(-w_{,xxx}+l^{2}w_{,xxxxx}\right)+H_{11}^{*}\left(\psi_{,xx}-l^{2}\psi_{,xxxx}\right)\right.\\&\left.-A_{44}^{*}\left(\psi-l^{2}\psi_{,xx}\right)=I_{3}\left(w_{,xtt}-\mu^{2}w_{,xxxtt}\right)+I_{4}\left(\psi_{,tt}-\mu^{2}\psi_{,xxtt}\right)\right)\end{aligned}\tag{15c}$$

where

$$\begin{aligned}\Gamma_{1}&=u_{,xx}w_{,x}+u_{,x}w_{,xx}+(3/2)w_{,xx}w_{,x}^{2}\\\Gamma_{2}&=u_{,xxxx}w_{,x}+u_{,xxx}w_{,xx}+4w_{,x}w_{,xx}w_{,xxx}+\left(w_{,xx}+w_{,xxxx}\right)w_{,x}^{2}\\\Gamma_{3}&=u_{,xxxx}w_{,x}+3u_{,xxx}w_{,xx}+3u_{,xx}w_{,xxx}+u_{,x}w_{,xxxx}+3w_{,xx}^{3}+9w_{,x}w_{,xx}w_{,xxx}+(3/2)w_{,x}^{2}w_{,xxxx}\\\Gamma_{4}&=u_{,xxxxx}w_{,x}+3u_{,xxxx}w_{,xx}+3u_{,xxx}w_{,xxx}+u_{,xx}w_{,xxxx}+8w_{,xx}w_{,xxx}^{2}+10w_{,xxx}w_{,xx}^{2}\\&\quad+4w_{,xx}w_{,xxx}^{2}+14w_{,x}w_{,xxx}w_{,xxxx}+8w_{,x}w_{,xx}w_{,xxxx}+6w_{,x}w_{,xx}w_{,xxx}\\&\quad+\left(w_{,xxxx}+w_{,xxxxx}\right)w_{,x}^{2}+2w_{,xx}^{3}\end{aligned}\tag{16}$$

in which

In order to perform the numerical solving process in a more general form, the following dimensionless parameters are taken into consideration

$$X=\frac{x}{L},\ U=\frac{u}{h},\ W=\frac{w}{h},\ \Psi=\psi,\ \eta_{1}=\frac{l}{L},\ \eta_{2}=\frac{\mu}{L},\ \beta=\frac{h}{L}$$

$$T=\frac{t}{L}\sqrt{\frac{A_{11}^{*}}{I_{0}}},$$

$$\left\{a_{11}^{*},a_{44}^{*},d_{11}^{*},f_{11}^{*},h_{11}^{*}\right\}=\left\{\frac{A_{11}^{*}}{A_{11}^{*}},\frac{A_{44}^{*}}{A_{11}^{*}},\frac{D_{11}^{*}}{A_{11}^{*}h^{2}},\frac{F_{11}^{*}}{A_{11}^{*}h^{2}},\frac{H_{11}^{*}}{A_{11}^{*}h^{2}}\right\}\tag{17}$$

$$\left\{I_{0}^{*},I_{2}^{*},I_{3}^{*},I_{4}^{*}\right\}=\left\{\frac{I_{0}}{I_{0}},\frac{I_{2}}{I_{0}h^{2}},\frac{I_{3}}{I_{0}h^{2}},\frac{I_{4}}{I_{0}h^{2}}\right\},$$

$$\mathcal{Q}=\frac{qL^{2}}{A_{11}^{*}h},\ \left\{K_{1},K_{2}\right\}=\left\{\frac{L^{4}k_{1}}{A_{11}^{*}h^{2}},\frac{L^{2}k_{2}}{A_{11}^{*}h^{2}}\right\}$$

As a result, the dimensionless form of the size-dependent governing differential equations of motion can be constructed as

$$a_{11}^{*}\left[U_{,XX}+\beta W_{,X}W_{,XX}-\eta_{1}^{2}\left(U_{,XXXX}+3\beta W_{,XX}W_{,XXX}+\beta W_{,X}W_{,XXXX}\right)\right]=I_{0}^{*}\left(U_{,TT}-\eta_{2}^{2}U_{,XXTT}\right)\tag{18a}$$

$$\begin{aligned}&d_{11}^{*}\left(W_{,XXXX}-\eta_{1}^{2}W_{,XXXXXX}\right)-f_{11}^{*}\left(\Psi_{,XXX}-\eta_{1}^{2}\Psi_{,XXXXX}\right)+K_{1}\left(W-\eta_{2}^{2}W_{,XX}\right)\\&\quad-K_{2}\left(W_{,XX}-\eta_{2}^{2}W_{,XXXX}\right)-a_{11}^{*}\tilde{\Gamma}_{1}+\eta_{1}^{2}a_{11}^{*}\tilde{\Gamma}_{2}+\eta_{2}^{2}a_{11}^{*}\tilde{\Gamma}_{3}-\eta_{1}^{2}\eta_{2}^{2}a_{11}^{*}\tilde{\Gamma}_{4}\\&\quad=\mathcal{Q}-\eta_{2}^{2}\mathcal{Q}_{,XX}-I_{0}^{*}\left(W_{,TT}-\eta_{2}^{2}W_{,XXTT}\right)+I_{2}^{*}\left(W_{,XXTT}-\eta_{2}^{2}W_{,XXXXTT}\right)\\&\quad+I_{3}^{*}\left(\Psi_{,XTT}-\eta_{2}^{2}\Psi_{,XXXTT}\right)\end{aligned}\tag{18b}$$

$$\begin{aligned}&f_{11}^{*}\left(W_{,XXX}-\eta_{1}^{2}W_{,XXXXX}\right)-h_{11}^{*}\left(\Psi_{,XX}-\eta_{1}^{2}\Psi_{,XXXX}\right)\\&+a_{44}^{*}\left(\Psi-\eta_{1}^{2}\Psi_{,XX}\right)=-I_{3}^{*}\left(W_{,XTT}-\eta_{2}^{2}W_{,XXXTT}\right)\\&-I_{4}^{*}\left(\Psi_{,TT}-\eta_{2}^{2}\Psi_{,XXTT}\right)\end{aligned}\tag{18c}$$

$$\begin{aligned}\tilde{\Gamma}_{1}&=\beta U_{,XX}W_{,X}+\beta U_{,X}W_{,XX}+(3/2)\beta^{2}W_{,XX}W_{,X}^{2}\\\tilde{\Gamma}_{2}&=\beta U_{,XXXX}W_{,X}+\beta U_{,XXX}W_{,XX}+4\beta^{2}W_{,X}W_{,XX}W_{,XXX}\\&\quad+\beta^{2}\left(W_{,XX}+W_{,XXXX}\right)W_{,X}^{2}\\\tilde{\Gamma}_{3}&=\beta\left[U_{,XXXX}W_{,X}+3U_{,XXX}W_{,XX}+3U_{,XX}W_{,XXX}+U_{,X}W_{,XXXX}\right]\\&\quad+\beta^{2}\left[3W_{,XX}^{3}+9W_{,X}W_{,XX}W_{,XXX}+(3/2)W_{,X}^{2}W_{,XXXX}\right]\\\tilde{\Gamma}_{4}&=\beta\left[U_{,XXXXXX}W_{,X}+3U_{,XXXXX}W_{,XX}+3U_{,XXXX}W_{,XXX}+U_{,XXX}W_{,XXXX}\right]\\&\quad+\beta^{2}\left[10W_{,XXXX}W_{,XX}^{2}+12W_{,XX}W_{,XXX}^{2}+14W_{,X}W_{,XXX}W_{,XXXX}\right.\\&\quad+8W_{,X}W_{,XX}W_{,XXXXX}+6W_{,X}W_{,XX}W_{,XXX}\\&\quad\left.+\left(W_{,XXXX}+W_{,XXXXX}\right)W_{,X}^{2}+2W_{,XX}^{3}\right]\end{aligned}\tag{19}$$

3 Numerical solution methodology

The nonlocal strain gradient governing equations of motion are solved numerically with the aid of a solution methodology based upon the GDQ method together with the Galerkin technique [76–78]. Consequently, in order to discretize X domain, the shifted Chebyshev–Gauss–Lobatto grid point is put to use as below

$$X_{i}=(1/2)\left[1-\cos\left(\pi(i-1)/(n-1)\right)\right],\quad i=1,2,3,\ldots,n\tag{20}$$

Thereby, the discretized governing equations of motion can be written in terms of mass matrix, damping matrix and stiffness matrix as below

$$\mathcal{M}\ddot{\mathbf{p}} + \mathcal{C}\dot{\mathbf{p}} + \mathcal{K}_L\mathbf{p} + \mathcal{K}_N = \mathcal{Q}\cos(\Omega T) \tag{21}$$

where

$$\mathbf{U} = \begin{bmatrix} U_1 \\ U_2 \\ U_3 \\ \vdots \\ U_n \end{bmatrix},\ \mathbf{W} = \begin{bmatrix} W_1 \\ W_2 \\ W_3 \\ \vdots \\ W_n \end{bmatrix},\ \mathbf{\Psi} = \begin{bmatrix} \Psi_1 \\ \Psi_2 \\ \Psi_3 \\ \vdots \\ \Psi_n \end{bmatrix} \tag{23}$$

$$\mathbf{p} = \begin{bmatrix} \mathbf{U}^{\mathrm{T}} \\ \mathbf{W}^{\mathrm{T}} \\ \mathbf{\Psi}^{\mathrm{T}} \end{bmatrix}_{3\times n}$$

$$\mathcal{M} = \begin{bmatrix} -I_0^*\left(\mathcal{D}_X^{(0)} - \eta_2^2\mathcal{D}_X^{(2)}\right) & 0 & 0 \\ 0 & I_0^*\left(\mathcal{D}_X^{(0)} - \eta_2^2\mathcal{D}_X^{(2)}\right) - I_2^*\left(\mathcal{D}_X^{(2)} - \eta_2^2\mathcal{D}_X^{(4)}\right) & -I_3^*\left(\mathcal{D}_X^{(1)} - \eta_2^2\mathcal{D}_X^{(3)}\right) \\ 0 & I_3^*\left(\mathcal{D}_X^{(1)} - \eta_2^2\mathcal{D}_X^{(3)}\right) & I_4^*\left(\mathcal{D}_X^{(0)} - \eta_2^2\mathcal{D}_X^{(2)}\right) \end{bmatrix}$$

$$\mathcal{K}_L = \begin{bmatrix} a_{11}^*\left(\mathcal{D}_X^{(2)} - \eta_1^2\mathcal{D}_X^{(4)}\right) & 0 & 0 \\ 0 & a_{11}^*\left(\mathcal{D}_X^{(4)} - \eta_1^2\mathcal{D}_X^{(6)}\right) + K_1\left(1 - \eta_2^2\mathcal{D}_X^{(2)}\right) - K_2\left(\mathcal{D}_X^{(2)} - \eta_2^2\mathcal{D}_X^{(4)}\right) & -f_{11}^*\left(\mathcal{D}_X^{(3)} - \eta_1^2\mathcal{D}_X^{(5)}\right) \\ 0 & f_{11}^*\left(\mathcal{D}_X^{(3)} - \eta_1^2\mathcal{D}_X^{(5)}\right) & a_{44}^*\left(\mathcal{D}_X^{(0)} - \eta_1^2\mathcal{D}_X^{(2)}\right) - h_{11}^*\left(\mathcal{D}_X^{(2)} - \eta_1^2\mathcal{D}_X^{(4)}\right) \end{bmatrix} \tag{22}$$

$$\mathcal{K}_N = \begin{bmatrix} k_N^u \\ k_N^w \\ 0 \end{bmatrix}_{3\times n}, \quad \mathcal{Q}^{\mathrm{T}} = \begin{bmatrix} 0 & q & 0 \\ 0 & q & 0 \\ 0 & q & 0 \\ \vdots & \vdots & \vdots \\ 0 & q & 0 \end{bmatrix}_{n\times 3}$$

$$\mathcal{C} = (2c/\omega_L)\mathcal{K}_L$$

in which

$$k_N^u = a_{11}^*\beta\left(\mathcal{D}_X^{(1)}\mathbf{W}\right)\circ\left(\mathcal{D}_X^{(2)}\mathbf{W}\right) - 3a_{11}^*\eta_1^2\beta\left(\mathcal{D}_X^{(2)}\mathbf{W}\right)\circ\left(\mathcal{D}_X^{(3)}\mathbf{W}\right) - a_{11}^*\eta_1^2\beta\left(\mathcal{D}_X^{(1)}\mathbf{W}\right)\circ\left(\mathcal{D}_X^{(4)}\mathbf{W}\right)$$

$$\begin{aligned} k_N^w = &-a_{11}^*\beta\left[\left(\mathcal{D}_X^{(2)}\mathbf{U}\right)\circ\left(\mathcal{D}_X^{(1)}\mathbf{W}\right) + \left(\mathcal{D}_X^{(1)}\mathbf{U}\right)\circ\left(\mathcal{D}_X^{(2)}\mathbf{W}\right)\right] - (3/2)a_{11}^*\beta^2\left(\mathcal{D}_X^{(2)}\mathbf{W}\right)\circ\left(\mathcal{D}_X^{(1)}\mathbf{W}\right) \\ &\circ\left(\mathcal{D}_X^{(1)}\mathbf{W}\right) + a_{11}^*\eta_1^2\beta\left[\left(\mathcal{D}_X^{(4)}\mathbf{U}\right)\circ\left(\mathcal{D}_X^{(1)}\mathbf{W}\right) + 3\left(\mathcal{D}_X^{(3)}\mathbf{U}\right)\circ\left(\mathcal{D}_X^{(2)}\mathbf{W}\right)\right] \\ &+ a_{11}^*\eta_1^2\beta^2\left[4\left(\mathcal{D}_X^{(1)}\mathbf{W}\right)\circ\left(\mathcal{D}_X^{(2)}\mathbf{W}\right)\circ\left(\mathcal{D}_X^{(3)}\mathbf{W}\right) + \left(\mathcal{D}_X^{(2)}\mathbf{W}\right)\circ\left(\mathcal{D}_X^{(1)}\mathbf{W}\right)\circ\left(\mathcal{D}_X^{(1)}\mathbf{W}\right)\right. \\ &\left.+ \left(\mathcal{D}_X^{(4)}\mathbf{W}\right)\circ\left(\mathcal{D}_X^{(1)}\mathbf{W}\right)\circ\left(\mathcal{D}_X^{(1)}\mathbf{W}\right)\right] \\ &+ a_{11}^*\eta_2^2\beta\left[\left(\mathcal{D}_X^{(4)}\mathbf{U}\right)\circ\left(\mathcal{D}_X^{(1)}\mathbf{W}\right) + 3\left(\mathcal{D}_X^{(3)}\mathbf{U}\right)\circ\left(\mathcal{D}_X^{(2)}\mathbf{W}\right) + 3\left(\mathcal{D}_X^{(2)}\mathbf{U}\right)\circ\left(\mathcal{D}_X^{(3)}\mathbf{W}\right)\right. \\ &\left.+ \left(\mathcal{D}_X^{(1)}\mathbf{U}\right)\circ\left(\mathcal{D}_X^{(4)}\mathbf{W}\right)\right] \\ &+ a_{11}^*\eta_2^2\beta^2\left[3\left(\mathcal{D}_X^{(2)}\mathbf{W}\right)\circ\left(\mathcal{D}_X^{(2)}\mathbf{W}\right)\circ\left(\mathcal{D}_X^{(2)}\mathbf{W}\right) + 9\left(\mathcal{D}_X^{(1)}\mathbf{W}\right)\circ\left(\mathcal{D}_X^{(2)}\mathbf{W}\right)\circ\left(\mathcal{D}_X^{(3)}\mathbf{W}\right)\right. \\ &\left.+ (3/2)\left(\mathcal{D}_X^{(1)}\mathbf{W}\right)\circ\left(\mathcal{D}_X^{(1)}\mathbf{W}\right)\circ\left(\mathcal{D}_X^{(4)}\mathbf{W}\right)\right] \\ &- a_{11}^*\eta_1^2\eta_2^2\beta\left[\left(\mathcal{D}_X^{(6)}\mathbf{U}\right)\circ\left(\mathcal{D}_X^{(1)}\mathbf{W}\right) + 3\left(\mathcal{D}_X^{(5)}\mathbf{U}\right)\circ\left(\mathcal{D}_X^{(2)}\mathbf{W}\right) + 3\left(\mathcal{D}_X^{(4)}\mathbf{U}\right)\circ\left(\mathcal{D}_X^{(3)}\mathbf{W}\right) + \left(\mathcal{D}_X^{(3)}\mathbf{U}\right)\circ\left(\mathcal{D}_X^{(4)}\mathbf{W}\right)\right] \\ &- a_{11}^*\eta_1^2\eta_2^2\beta^2\left[10\left(\mathcal{D}_X^{(4)}\mathbf{W}\right)\circ\left(\mathcal{D}_X^{(2)}\mathbf{W}\right)\circ\left(\mathcal{D}_X^{(2)}\mathbf{W}\right) + 12\left(\mathcal{D}_X^{(2)}\mathbf{W}\right)\circ\left(\mathcal{D}_X^{(3)}\mathbf{W}\right)\right. \\ &\circ\left(\mathcal{D}_X^{(3)}\mathbf{W}\right) + 14\left(\mathcal{D}_X^{(1)}\mathbf{W}\right)\circ\left(\mathcal{D}_X^{(3)}\mathbf{W}\right)\circ\left(\mathcal{D}_X^{(4)}\mathbf{W}\right) + 8\left(\mathcal{D}_X^{(1)}\mathbf{W}\right)\circ\left(\mathcal{D}_X^{(2)}\mathbf{W}\right) \\ &\circ\left(\mathcal{D}_X^{(5)}\mathbf{W}\right) + 6\left(\mathcal{D}_X^{(1)}\mathbf{W}\right)\circ\left(\mathcal{D}_X^{(2)}\mathbf{W}\right)\circ\left(\mathcal{D}_X^{(3)}\mathbf{W}\right) + \left(\mathcal{D}_X^{(4)}\mathbf{W}\right)\circ\left(\mathcal{D}_X^{(2)}\mathbf{W}\right)\circ\left(\mathcal{D}_X^{(2)}\mathbf{W}\right) \\ &\left.+ \left(\mathcal{D}_X^{(5)}\mathbf{W}\right)\circ\left(\mathcal{D}_X^{(2)}\mathbf{W}\right)\circ\left(\mathcal{D}_X^{(2)}\mathbf{W}\right) + 2\left(\mathcal{D}_X^{(2)}\mathbf{W}\right)\circ\left(\mathcal{D}_X^{(2)}\mathbf{W}\right)\circ\left(\mathcal{D}_X^{(2)}\mathbf{W}\right)\right] \end{aligned}$$

where c is the damping parameter, $\circ$ denotes the Hadamard product, and the derivative operators corresponding to each order can be introduced as

$$\left[D_X^{(i)}\right]_{kj} = \begin{cases} \left[\text{Identity matrix}\right]_{n\times n} & i=0 \\ \dfrac{\prod_{j=1,j\neq k}^{n}(X_k-X_j)}{(X_k-X_j)\prod_{k=1,k\neq j}^{n}(X_j-X_k)} & i=1,\ j,k=1,2,3,\ldots,n \\ i\left(\left[D_X^{(1)}\right]_{kj}\left[D_X^{(i-1)}\right]_{kk}-\dfrac{\left[D_X^{(i-1)}\right]_{kj}}{(X_k-X_j)}\right) & i=2,3,4,\ldots,n-1,\ j,k=1,2,3,\ldots,n \\ -\sum_{k=1,k=j}^{n}\left[D_X^{(i)}\right]_{kj} & i=1,2,3,\ldots,n-1,\ j,k=1,2,3,\ldots,n \end{cases} \tag{24}$$

In order to continue the solution methodology, the variable matrix $\mathbf{p}$ is expressed separately as below

$$\mathbf{p}(X,T)=\boldsymbol{\varphi}(X)g(T) \tag{25}$$

By inserting Eq. (25) in Eq. (21), one will have

$$\mathcal{M}\boldsymbol{\varphi}\ddot{g}+\mathcal{C}\boldsymbol{\varphi}\dot{g}+\mathcal{K}_L\boldsymbol{\varphi}g+\mathcal{K}_N=\mathcal{Q}\cos(\Omega T) \tag{26}$$

Thereafter, with the aid of the Galerkin technique, the Duffing-type equation of motion relevant to the forced oscillations of the lipid protein micro/nanotubule can be extracted as

$$\hat{\mathcal{M}}\ddot{\mathbf{g}}+\hat{\mathcal{C}}\dot{\mathbf{g}}+\hat{\mathcal{K}}_L\mathbf{g}+\hat{\mathcal{K}}_N\left(\mathbf{g}^3\right)=\hat{\mathcal{Q}}\cos(\Omega T) \tag{27}$$

in which

$$\hat{\mathcal{M}}=\boldsymbol{\varphi}^{\mathbf{T}}_{\text{diagonal}}\mathcal{M}\boldsymbol{\varphi},\ \hat{\mathcal{C}}=\boldsymbol{\varphi}^{\mathbf{T}}_{\text{diagonal}}\mathcal{C}\boldsymbol{\varphi},\ \hat{\mathcal{K}}_L=\boldsymbol{\varphi}^{\mathbf{T}}_{\text{diagonal}}\mathcal{K}_L\boldsymbol{\varphi}$$
$$\hat{\mathcal{K}}_N=\boldsymbol{\varphi}^{\mathbf{T}}_{\text{diagonal}}\mathcal{K}_N,\ \hat{\mathcal{Q}}=\boldsymbol{\varphi}^{\mathbf{T}}_{\text{diagonal}}\mathcal{Q} \tag{28}$$

It should be noted that the expressions for $\boldsymbol{\varphi}(X)$ corresponding to different boundary conditions are actually represent the associated linear vibrational mode shapes (eigenvectors) which can be obtained numerically for each type of boundary conditions.

Through definition of $\tilde{T}=\Omega T$, Eq. (28) can be rewritten as

$$\Omega^2\hat{\mathcal{M}}\ddot{\mathbf{g}}+\Omega\hat{\mathcal{C}}\dot{\mathbf{g}}+\hat{\mathcal{K}}_L\mathbf{g}+\hat{\mathcal{K}}_N\left(\mathbf{g}^3\right)=\hat{\mathcal{Q}}\cos\left(\tilde{T}\right) \tag{29}$$

Now, in order to discretize the time domain, it is assumed that

$$\tilde{T}_i=i/n_t\quad i=1,2,3,\ldots,n_t \tag{30}$$

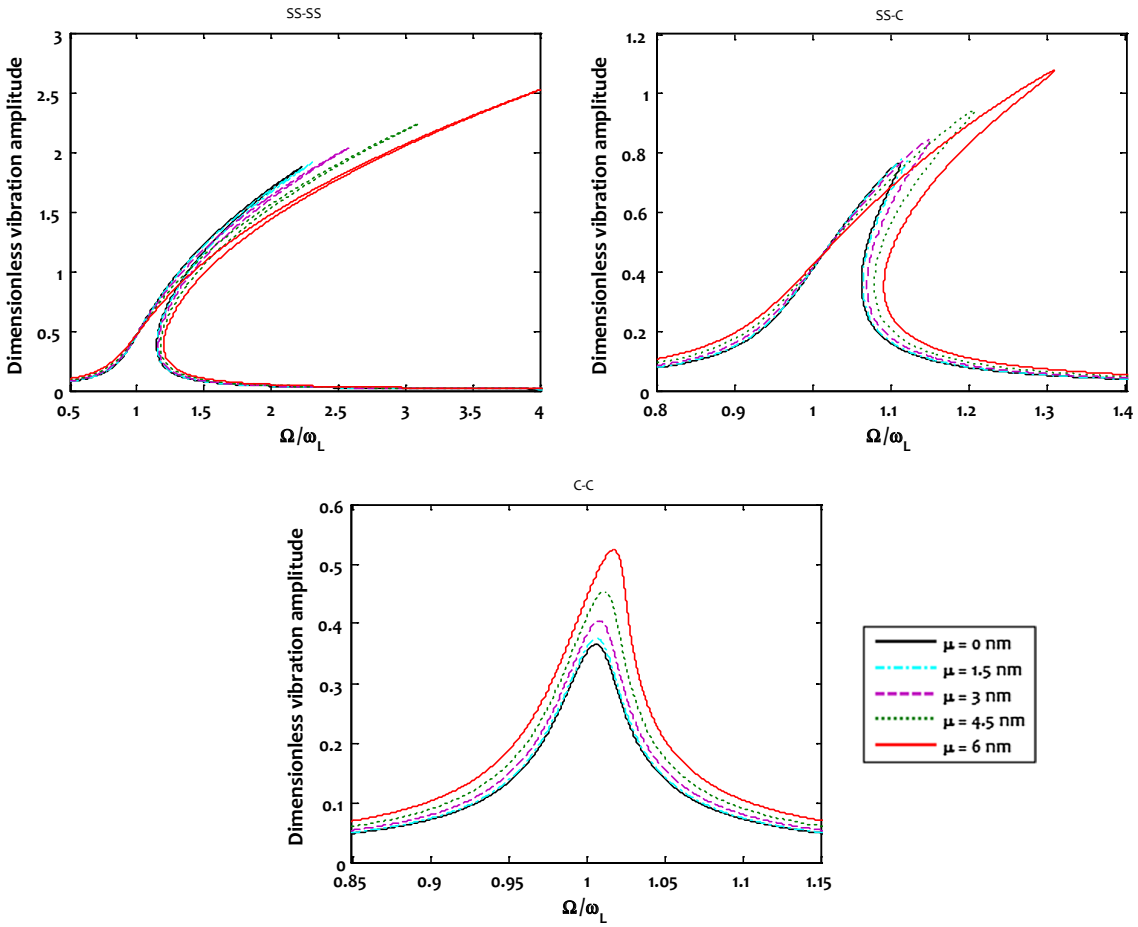

Fig. 2 Size-dependent frequency response of the protein micro/nanotubules corresponding to different nonlocal parameters

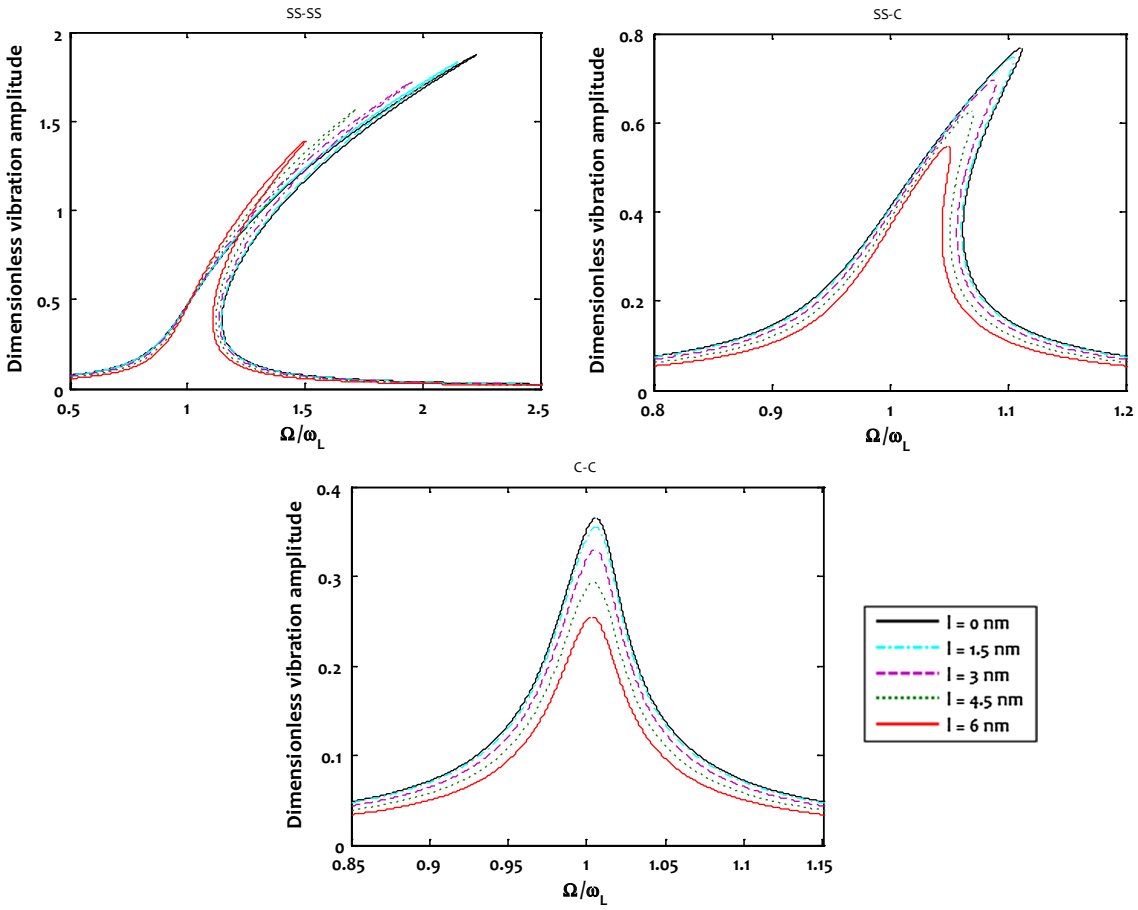

Fig. 3 Size-dependent frequency response of the protein micro/nanotubules corresponding to different strain gradient parameters

where n_t denotes the number of discrete points on the time domain and is an even number.

Consequently, it yields

$$\Omega^2\hat{\mathcal{M}}\left(\mathcal{D}_T^{(2)}\right)^{\mathrm{T}}\mathbf{G}+\Omega\hat{\mathcal{C}}\left(\mathcal{D}_T^{(1)}\right)^{\mathrm{T}}\mathbf{G}+\hat{\mathcal{K}}_L\mathbf{G}+\hat{\mathcal{K}}_N\left(\mathbf{G}^3\right)=\hat{\mathcal{Q}}\mathbf{S} \tag{31}$$

in which $\mathbf{G}$ includes the first m discretized mode shapes (eigenvectors) relevant to the Galerkin technique as

$$\mathbf{G}=\left[\begin{array}{cccccccccccc}[q_1^u]_{1\times n_t} & [q_2^u]_{1\times n_t} & \cdots & [q_m^u]_{1\times n_t} & [q_1^w]_{1\times n_t} & [q_2^w]_{1\times n_t} & \cdots & [q_m^w]_{1\times n_t} & [q_1^\psi]_{1\times n_t} & [q_2^\psi]_{1\times n_t} & \cdots & [q_m^\psi]_{1\times n_t}\end{array}\right]$$

and

$$\mathbf{S}=\left[\cos\left(\tilde{T}_1\right)\ \cos\left(\tilde{T}_2\right)\ \cdots\ \cos\left(\tilde{T}_{n_t}\right)\right] \tag{32}$$

Also, the time derivative operator corresponding to each order can be introduced explicitly in the following matrix forms

$$\mathcal{D}_T^{(1)}=\mathcal{G}_{ij}^{(1)}\ where$$

$$\begin{cases}\mathcal{G}_{11}^{(1)}=0\\ \mathcal{G}_{i1}^{(1)}=(-1)^{i-1}\cot\left(\frac{\pi(i-1)}{n_t}\right)\\ \mathcal{G}_{ij}^{(1)}=(-1)^{n_t+1-j}\cot\left(\frac{\pi(n_t+1-j)}{n_t}\right)\\ \mathcal{G}_{(i+1)(j+1)}^{(1)}=\mathcal{G}_{ij}^{(1)}\end{cases}\qquad i,j=2,3,\ldots,n_t \tag{33}$$

$$\mathcal{D}_T^{(2)}=\mathcal{G}_{ij}^{(2)}$$

$$\text{where}\begin{cases}\mathcal{G}_{11}^{(2)}=-\left(\frac{1}{6}+\frac{n_t^2}{12}\right)\\ \mathcal{G}_{i1}^{(2)}=(-1)^{i-1}/\left[2\sin^2\left(\frac{\pi(i-1)}{n_t}\right)\right]\\ \mathcal{G}_{ij}^{(2)}=(-1)^{n_t+1-j}/\left[2\sin^2\left(\frac{\pi(n_t+1-j)}{n_t}\right)\right]\\ \mathcal{G}_{(i+1)(j+1)}^{(2)}=\mathcal{G}_{ij}^{(2)}\end{cases}\qquad i,j=2,3,\ldots,n_t \tag{34}$$

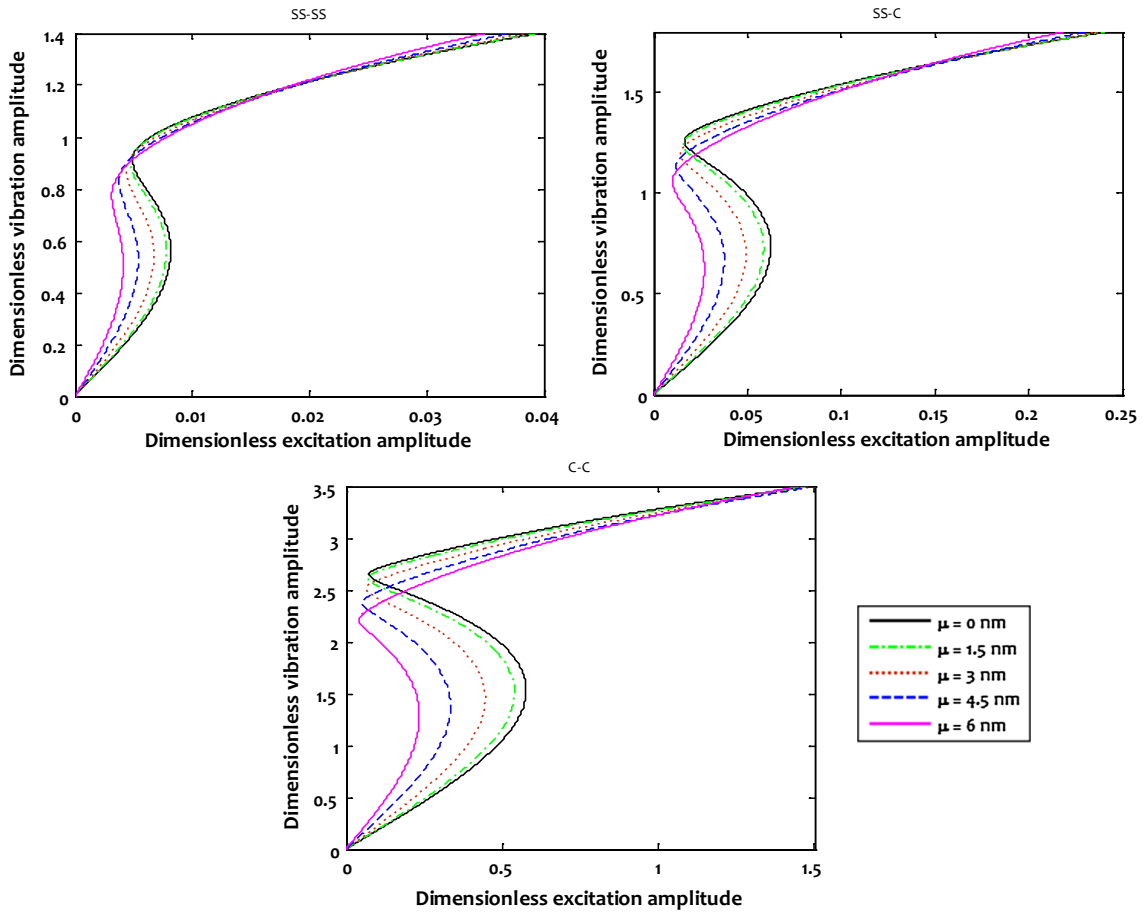

Fig. 4 Size-dependent amplitude response of the protein micro/nanotubules corresponding to different nonlocal parameters

Now, by vectorization of matrices $\mathbf{G}$ and $\hat{\mathcal{K}}_N$ [71–73], and using Kronecker product, the vectorized definition of Eq. (32) can be expressed as

$$\left(\Omega^2\left(\mathcal{D}_T^{(2)}\otimes\hat{\mathcal{M}}\right)+\Omega\left(\mathcal{D}_T^{(1)}\otimes\hat{C}\right)+\left(\boldsymbol{I}_t\otimes\hat{\mathcal{K}}_L\right)\right)vec(\mathbf{G})+vec\left(\hat{\mathcal{K}}_N\left(\mathbf{G}^3\right)\right)-\mathbf{S}\left(\boldsymbol{I}_t\otimes\hat{Q}\right)=0 \tag{35}$$

where $\boldsymbol{I}_t$ represents the identity matrix (zero order of the time derivative).

Finally, the pseudo-arc-length continuation method [79] is utilized to solve Eq. (35) as a set of nonlinear equations.

4 Numerical results and discussion

In this section, the nonlinear primary resonance of a lipid protein nanotubule with thickness of 1.6 nm, mid-radius of 10.7 nm and length of $L=20$ h is considered. Also, the material properties are considered as: $E=0.8$ GPa, $\nu=0.3$, and $\rho=1042$ kg/m^3 [80]. Three different boundary conditions, namely as simply supported–simply supported (SS–SS), simply supported–clamped (SS–C) and clamped–clamped (C–C), are considered for the two ends of the micro/nanotubule.

Figures 2 and 3 illustrate the size-dependent frequency response curves associated with the nonlinear primary resonance corresponding to various nonlocal parameters and strain gradient parameters, respectively. It is revealed that by taking the nonlocality into account, the peak of jump phenomenon for the vibration amplitude increases and it is shifted to higher excitation frequency. In other words, it means that the nonlocal size effect leads to increase the geometrical nonlinearity regarding to the nonlinear primary resonance of nanotubules. However, by changing the end supports from simply supported to clamped one, the significance of this pattern decreases. On the other hand, the strain gradient size dependency leads to reduce the peak of jump phenomenon for the vibration amplitude and it is shifted to lower excitation frequency. In other words, it means that the

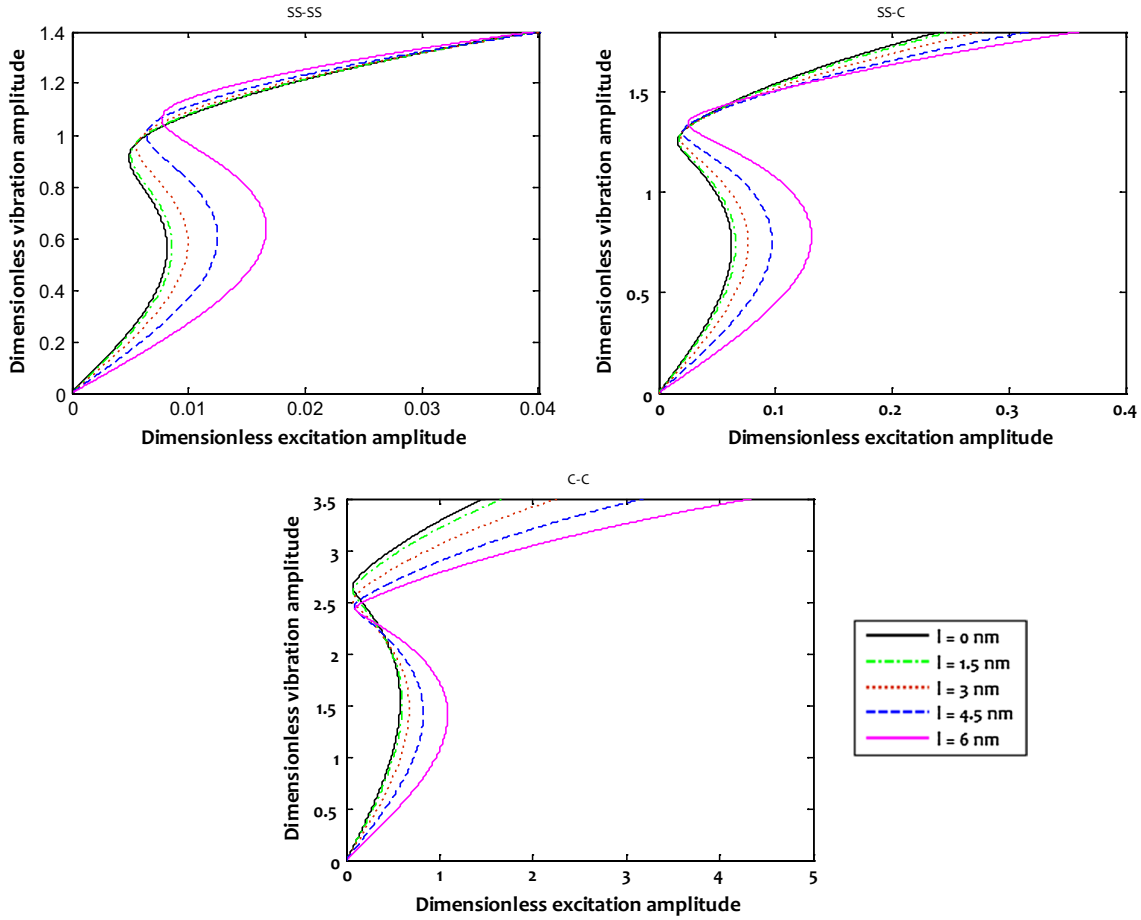

Fig. 5 Size-dependent amplitude response of the protein micro/nanotubules corresponding to different strain gradient parameters

Table 1 Dimensionless natural frequencies of a nanotubule corresponding to various values of the small-scale parameters and different boundary conditions

$\mu = 0$ nm $l = 0$ nm	$\mu = 1.5$ nm $l = 0$ nm	$\mu = 3$ nm $l = 0$ nm	$\mu = 6$ nm $l = 0$ nm	$\mu = 0$ nm $l = 1.5$ nm	$\mu = 0$ nm $l = 3$ nm	$\mu = 0$ nm $l = 6$ nm
SS–SS boundary conditions						
0.2671	0.2614 (−2.13%)	0.2457 (−8.01%)	0.1983 (−25.76%)	0.2728 (+2.13%)	0.2902 (+8.65%)	0.3597 (+34.67%)
C–SS boundary conditions						
0.6518	0.6357 (−2.47%)	0.5918 (−9.21%)	0.4638 (−28.84%)	0.6682 (+2.52%)	0.7177 (+10.11%)	0.9153 (+40.43%)
C–C boundary conditions						
1.3716	1.3353 (−2.65%)	1.2370 (−9.81%)	0.9557 (−30.32%)	1.4087 (+2.71%)	1.5200 (+13.83%)	1.9651 (+43.27%)

strain gradient size effect causes to decrease the geometrical nonlinearity regarding to the nonlinear primary resonance of nanotubules. It can be seen again that through changing the boundary conditions from SS–SS to C–C, the influence of the strain gradient size effect decreases.

In Figs. 4 and 5, the size-dependent amplitude response curves related to the nonlinear primary resonance of lipid nanotubule are depicted corresponding to various values of nonlocal and strain gradient parameters, respectively. It is observed that by increasing the excitation amplitude, the

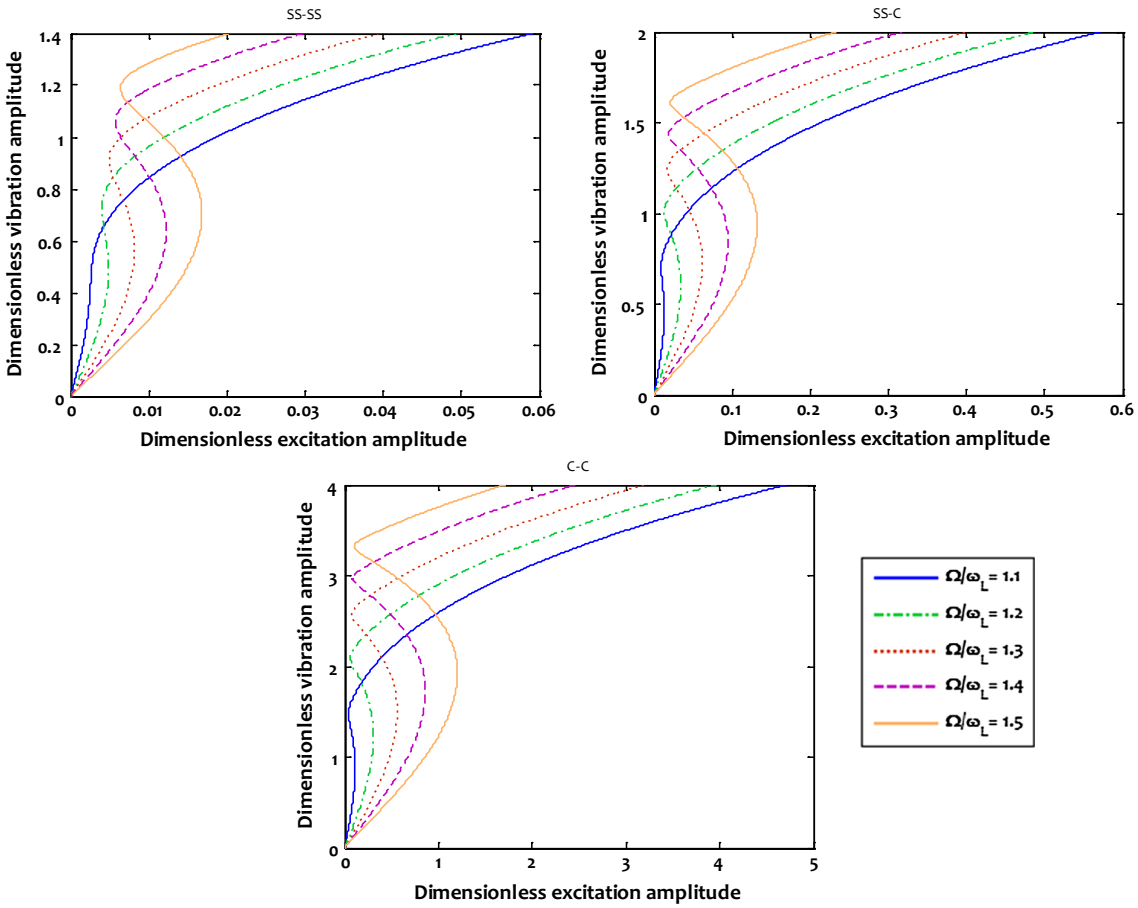

Fig. 6 Size-dependent amplitude response of the protein micro/nanotubules corresponding to different excitation frequencies

vibrational response amplitude increases up to the first bifurcation point. Thereafter, increase in the vibrational response amplitude continues through reduction in the excitation amplitude up to the second bifurcation point. It is found that the nonlocal size effect causes to decrease the excitation amplitudes associated with both of the bifurcation points, but its effect on the first one is more considerable. However, the strain gradient size dependency has an opposite influence and leads to increase them. Moreover, it is seen that by changing the end supports from the simply supported to the clamped one, the influence of the nonlocality on the excitation amplitude associated with the bifurcation points increases, but the influence of the strain gradient size dependency decreases.

In Table 1, the dimensionless natural frequencies of the nanotubule with different boundary conditions are tabulated corresponding to various values of the small-scale parameters. It is indicated that the nonlocal size effect leads to decrease the natural frequency, but the strain gradient size effect causes to increase it. However, the increment caused by the strain gradient size dependency is more than the reduction caused by the nonlocality.

Figure 6 represents the size-dependent amplitude response of the lipid nanotubule under different frequency ratios. It is revealed that by increasing the value of the excitation frequency, the excitation amplitudes associated with the bifurcation points increase. Also, it leads to increase the difference between the excitation amplitudes of the two bifurcation points, and this pattern becomes more significant by changing the boundary conditions from SS–SS to C–C. This observation may be related to this point that by changing the boundary conditions from SS–SS to C–C, the deflection of the excited nanotubule reduces.

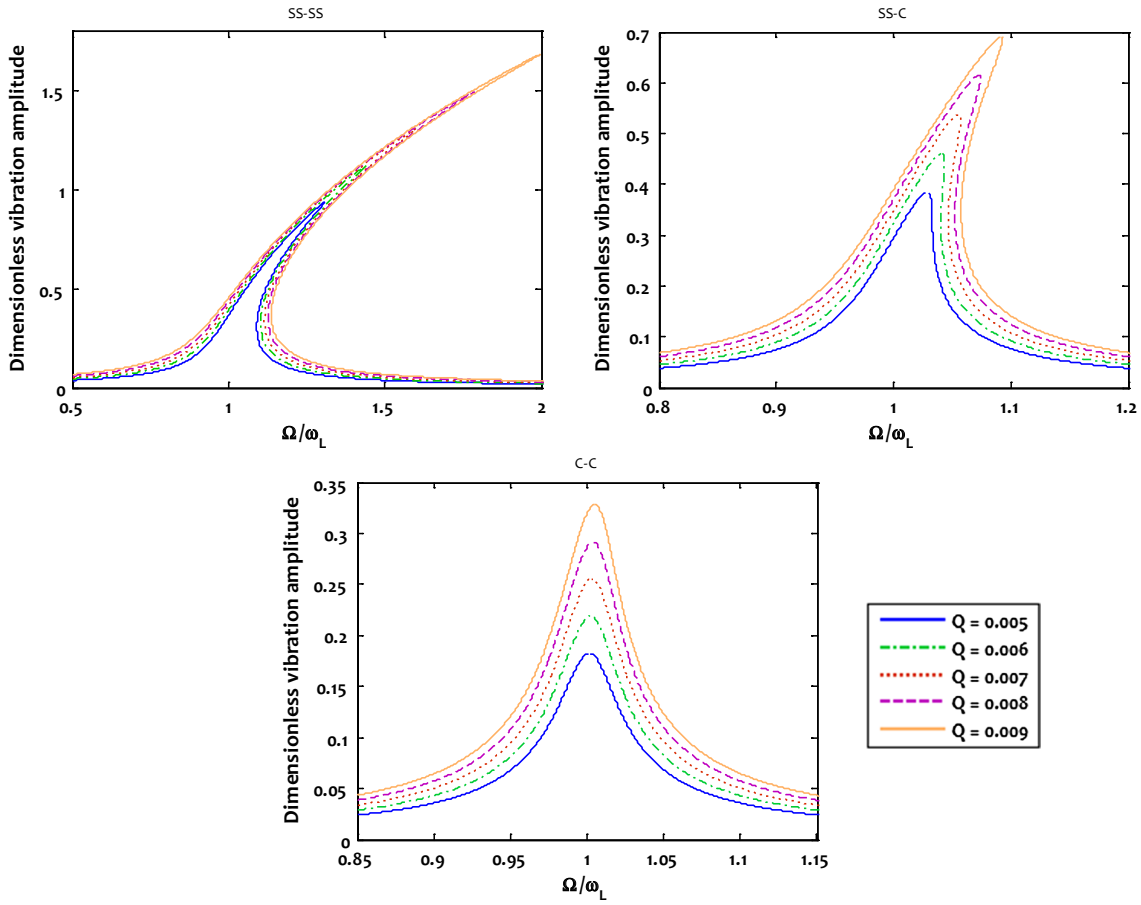

Fig. 7 Size-dependent frequency response of the protein micro/nanotubules corresponding to different excitation amplitudes

In Fig. 7, the size-dependent frequency response of the lipid nanotubule subjected to the soft excitations with various amplitudes is shown. It is indicated that through enhancement of the excitation amplitude, the peak of the jump phenomenon associated with the frequency response of nanotubule increases. This pattern is more significant for simply supported end conditions than clamped one, which may be related to higher deflection of a nanotubule with simply supported boundary conditions.

Figures 8 and 9 demonstrate, respectively, the frequency response and amplitude response of the lipid nanotubule embedded on a different biomedium. It is obvious that by taking the elastic biomedium into consideration, the peak of the jump phenomenon related to the frequency response decreases, especially for SS–SS boundary conditions, due to this fact that the elastic foundation causes to reduce the deflection of the excited nanotubule. However, it is seen that the excitation amplitudes associated with the bifurcation points increase. Moreover, it is displayed that this pattern is more significant for Pasternak type of biomedium including shear stiffness than the Winkler one.

5 Concluding remarks

The prime objective of the current study was to predict the nonlinear primary resonance of a lipid protein micro/nanotubule in the presence of the nonlocality and strain gradient size dependency. To accomplish this purpose, the nonlocal strain gradient elasticity theory was utilized within the framework of the refined hyperbolic shear deformation beam theory. Through the numerical solving process, the size-dependent frequency response and amplitude response

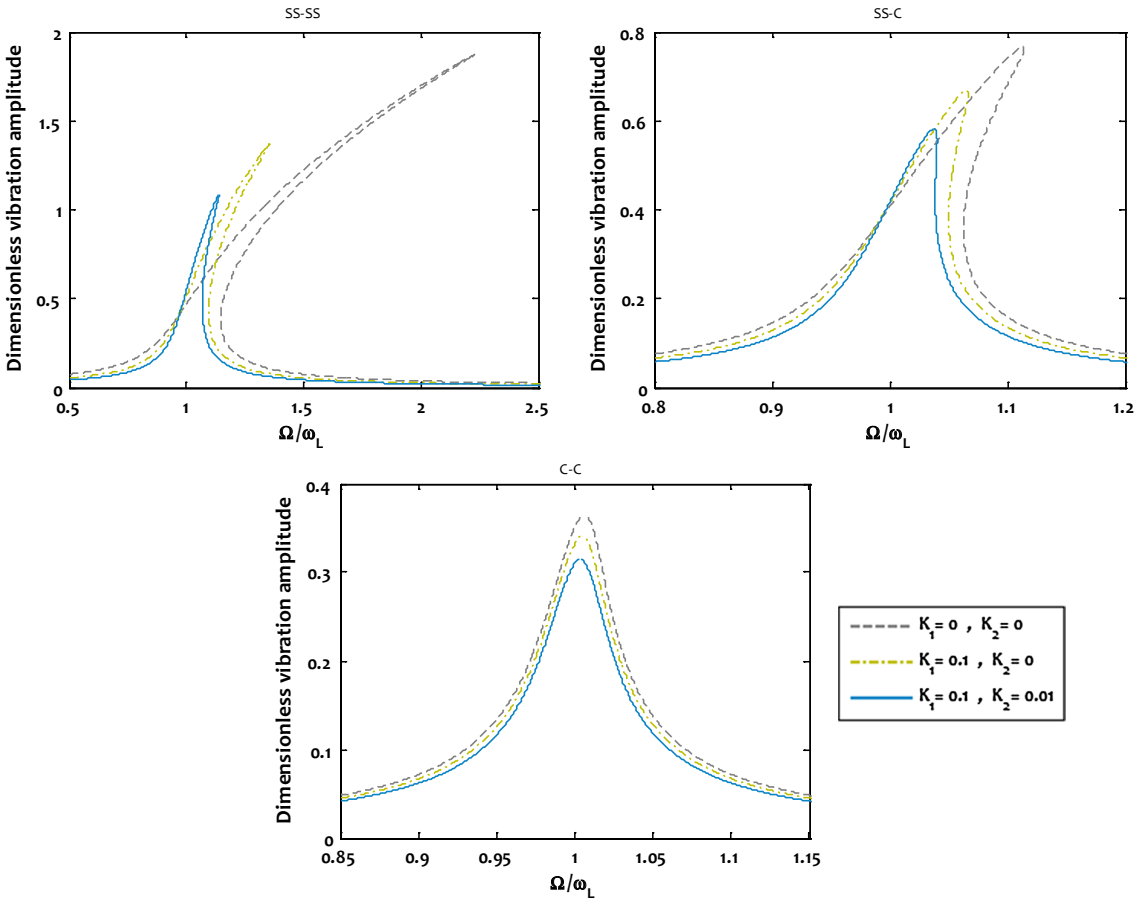

Fig. 8 Influence of the elastic biomedium on the size-dependent frequency response of the protein micro/nanotubules

of the lipid micro/nanotubule were obtained corresponding to different small-scale parameters.

It was observed that by taking the nonlocality into account, the peak of jump phenomenon for the vibration amplitude increases and it is shifted to higher excitation frequency. However, the strain gradient size dependency leads to reduce the peak of jump phenomenon for the vibration amplitude and it is shifted to lower excitation frequency.

It was indicated that by changing the boundary conditions from SS–SS to C–C, the influence of the size effects on the frequency response of lipid protein micro/nanotubule reduces. In addition, it was seen that by increasing the excitation amplitude, the vibrational response amplitude increases up to the first bifurcation point. Thereafter, increase in the vibrational response amplitude continues through reduction in the excitation amplitude up to the second bifurcation point.

It was seen that the nonlocal size effect causes to decrease the excitation amplitudes associated with both bifurcation points, but its effect on the first one is more considerable. However, the strain gradient size dependency has an opposite influence and leads to increase them.

It was displayed that by increasing the value of the excitation frequency, the excitation amplitudes associated with the bifurcation points increase. It was also demonstrated that by taking the elastic biomedium into consideration, the peak of the jump phenomenon related to the frequency response decreases, especially for SS–SS boundary conditions, but the excitation amplitudes associated with the bifurcation points increase.

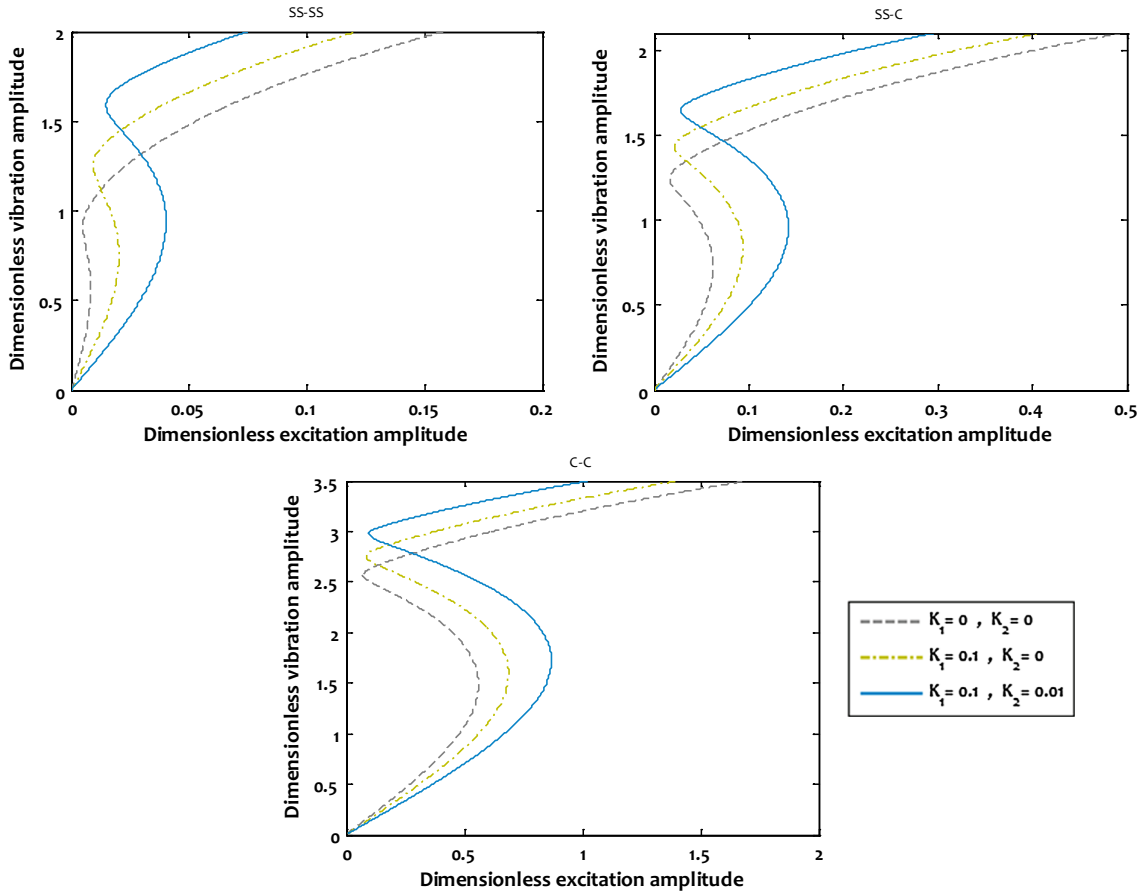

Fig. 9 Influence of the elastic biomedium on the size-dependent amplitude response of the protein micro/nanotubules

Compliance with ethical standards

Conflict of interest It is confirmed that there is no conflict of interest.

References

1. Zheng J, Buxbaum RE, Heidemann SR (1993) Investigation of microtubule assembly and organization accompanying tension-induced neurite initiation. J Cell Sci 104:1239–1250
2. Omelchanko T, Vasiliev JM, Gelfand IM, Feder HH, Bonder EM (2002) Mechanisms of polarization of the shape of fibroblasts and epitheliocytes: separation of the roles of microtubules and Rho-dependent actin–myosin contractility. Proc Natl Acad Sci USA 99:10452–10457
3. Gupton SL, Salmon WC, Waterman-Storer CM (2002) Converging populations of f-actin promote breakage of associated microtubules to spatially regulate microtubule turnover in migrating cells. Curr Biol 12:1891–1899
4. Pokorny J, Hasek J, Jelinek F (2005) Electromagnetic field of microtubules: effects on transfer of mass particles and electrons. J Biol Phys 31:501–514
5. Pokorny J, Hasek J, Vanis J, Jelinek F (2008) Biophysical aspects of cancer-electromagnetic mechanism. Indian J Exp Biol 46:310–321
6. Atanasov AT (2014) Calculation of vibration modes of mechanical waves on microtubules presented like strings and bars. Am J Mod Phys 3:1–11
7. Thai H-T, Vo TP (2012) A nonlocal sinusoidal shear deformation beam theory with application to bending, buckling and vibration of nanobeams. Int J Eng Sci 54:58–66
8. Wang L, Xu YY, Ni Q (2013) Size-dependent vibration analysis of three-dimensional cylindrical microbeams based on modified couple stress theory: a unified treatment. Int J Eng Sci 68:1–10
9. Liu C, Ke LL, Wang YS, Yang J, Kitipornchai S (2014) Buckling and post-buckling of size-dependent piezoelectric Timoshenko nanobeams subject to thermo-electro-mechanical loadings. Int J Struct Stab Dyn 14:1350067
10. Shojaeian M, Tadi Beni Y (2015) Size-dependent electromechanical buckling of functionally graded electrostatic nano-bridges. Sens Actuators, A 232:49–52
11. Sarvestani HY, Ghayoor H (2015) Free vibration analysis of curved nanotube structures. Int J Non Linear Mech 86:167–173
12. Sahmani S, Aghdam MM, Bahrami M (2015) On the postbuckling behavior of geometrically imperfect cylindrical nanoshells subjected to radial compression including surface stress effects. Compos Struct 131:414–424
13. Sahmani S, Aghdam MM, Bahrami M (2015) Nonlinear buckling and postbuckling behavior of cylindrical nanoshells subjected to combined axial and radial compressions incorporating surface stress effects. Compos B Eng 79:676–691

14. Sahmani S, Bahrami M, Aghdam MM (2015) Surface stress effects on the postbuckling behavior of geometrically imperfect cylindrical nanoshells subjected to combined axial and radial compressions. Int J Mech Sci 100:1–22
15. Nami MR, Janghorban M (2015) Free vibration analysis of rectangular nanoplates based on two-variable refined plate theory using a new strain gradient elasticity theory. J Braz Soc Mech Sci Eng 37:313–324
16. Shaat M, Abdelkefi A (2016) Size dependent and micromechanical modeling of strain gradient-based nanoparticle composite plates with surface elasticity. Eur J Mech A Solids 58:54–68
17. Akbarzadeh Khorshidi M, Shariati M (2016) Free vibration analysis of sigmoid functionally graded nanobeams based on a modified couple stress theory with general shear deformation theory. J Braz Soc Mech Sci Eng 38:2607–2619
18. Sahmani S, Bahrami M, Aghdam MM (2016) Surface stress effects on the nonlinear postbuckling characteristics of geometrically imperfect cylindrical nanoshells subjected to axial compression. Int J Eng Sci 99:92–106
19. Sahmani S, Aghdam MM, Bahrami M (2016) Size-dependent axial buckling and postbuckling characteristics of cylindrical nanoshells in different temperatures. Int J Mech Sci 107:170–179
20. Mohammadimehr M, Rousta Navi B, Ghorbanpour Arani A (2016) Modified strain gradient Reddy rectangular plate model for biaxial buckling and bending analysis of double-coupled piezoelectric polymeric nanocomposite reinforced by FG-SWNT. Compos B Eng 87:132–148
21. Zeighampour H, Shojaeian M (2017) Size-dependent vibration of sandwich cylindrical nanoshells with functionally graded material based on the couple stress theory. J Braz Soc Mech Sci Eng 39:2789–2800
22. Tavakolian F, Farrokhabadi A, Mirzaei M (2017) Pull-in instability of double clamped microbeams under dispersion forces in the presence of thermal and residual stress effects using nonlocal elasticity theory. Microsyst Technol 23:839–848
23. Sahmani S, Aghdam MM, Bahrami M (2017) An efficient size-dependent shear deformable shell model and molecular dynamics simulation for axial instability analysis of silicon nanoshells. J Mol Graph Model 77:263–279
24. Sahmani S, Aghdam MM, Bahrami M (2017) Nonlinear buckling and postbuckling behavior of cylindrical shear deformable nanoshells subjected to radial compression including surface free energy effects. Acta Mech Solida Sin 30:209–222
25. Lotfi M, Moghimi Zand M, Hosseini II, Baghani M, Dargazany R (2017) Transient behavior and dynamic pull-in instability of electrostatically-actuated fluid-conveying microbeams. Microsyst Technol 23:6015–6023
26. Farajpour A, Rastgoo A, Mohammadi M (2017) Vibration, buckling and smart control of microtubules using piezoelectric nanoshells under electric voltage in thermal environment. Phys B 509:100–114
27. Wang Y-G, Song H-F, Lin W-H, Xu L (2017) Large deflection analysis of functionally graded circular microplates with modified couple stress effect. J Braz Soc Mech Sci Eng 39:981–991
28. Sahmani S, Aghdam MM (2017) Size-dependent nonlinear bending of micro/nano-beams made of nanoporous biomaterials including a refined truncated cube cell. Phys Lett A 381:3818–3830
29. Sahmani S, Aghdam MM (2017) Nonlocal strain gradient beam model for nonlinear vibration of prebuckled and postbuckled multilayer functionally graded GPLRC nanobeams. Compos Struct 179:77–88
30. Ebrahimi F, Haghi P (2017) Wave propagation analysis of rotating thermoelastically-actuated nanobeams based on nonlocal strain gradient theory. Acta Mech Solida Sin 30:647–657
31. Fathi M, Ghassemi A (2017) The effects of surface stress and nonlocal small scale on the uniaxial and biaxial buckling of the rectangular piezoelectric nanoplate based on the two variable-refined plate theory. J Braz Soc Mech Sci Eng 39:3203–3216
32. Fattahi AM, Sahmani S (2017) Size dependency in the axial postbuckling behavior of nanopanels made of functionally graded material considering surface elasticity. Arab J Sci Eng 42:4617–4633
33. Imani Aria A, Biglari H (2018) Computational vibration and buckling analysis of microtubule bundles based on nonlocal strain gradient theory. Appl Math Comput 321:313–332
34. Mehralian F, Tadi Beni Y (2018) Vibration analysis of size-dependent bimorph functionally graded piezoelectric cylindrical shell based on nonlocal strain gradient theory. J Braz Soc Mech Sci Eng 40(27):1–15
35. Jiang J, Wang L (2018) Analytical solutions for thermal vibration of nanobeams with elastic boundary conditions. Acta Mech 229:2203–2219
36. Sahmani S, Aghdam MM (2018) Nonlocal strain gradient shell model for axial buckling and postbuckling analysis of magneto-electro-elastic composite nanoshells. Compos B Eng 132:258–274
37. Sahmani S, Aghdam MM (2018) Thermo-electro-radial coupling nonlinear instability of piezoelectric shear deformable nanoshells via nonlocal elasticity theory. Microsyst Technol 24:1333–1346
38. Sahmani S, Fattahi AM (2018) Development of efficient size-dependent plate models for axial buckling of single-layered graphene nanosheets using molecular dynamics simulation. Microsyst Technol 24:1265–1277
39. Mohammadi M, Eghtesad M, Mohammadi H (2018) Stochastic analysis of pull-in instability of geometrically nonlinear size-dependent FGM micro beams with random material properties. Compos Struct 200:466–479
40. Ma LH, Ke LL, Reddy JN, Yang J, Kitipornchai S, Wang YS (2018) Wave propagation characteristics in magneto-electro-elastic nanoshells using nonlocal strain gradient theory. Compos Struct 199:10–23
41. Sahmani S, Aghdam MM (2018) Small scale effects on the large amplitude nonlinear vibrations of multilayer functionally graded composite nanobeams reinforced with graphene-nanoplatelets. Int J Nanosci Nanotechnol 14:207–227
42. Sahmani S, Aghdam MM (2018) Boundary layer modeling of nonlinear axial buckling behavior of functionally graded cylindrical nanoshells based on the surface elasticity theory. Iran J Sci Technol Trans Mech Eng 42:229–245
43. Sahmani S, Fotouhi M, Aghdam MM (2018) Size-dependent nonlinear secondary resonance of micro-/nano-beams made of nanoporous biomaterials including truncated cube cells. Acta Mech. https://doi.org/10.1007/s00707-018-2334-9
44. Wang J, Shen H, Zhang B, Liu J, Zhang Y (2018) Complex modal analysis of transverse free vibrations for axially moving nanobeams based on the nonlocal strain gradient theory. Physica E 101:85–93
45. Sahmani S, Fattahi AM, Ahmed NA (2018) Nonlinear torsional buckling and postbuckling analysis of cylindrical silicon nanoshells incorporating surface free energy effects. Microsyst Technol. https://doi.org/10.1007/s00542-018-4246-y
46. Sahmani S, Fattahi AM, Ahmed NA (2018) Analytical mathematical solution for vibrational response of postbuckled laminated FG-GPLRC nonlocal strain gradient micro-/nanobeams. Eng Comput. https://doi.org/10.1007/s00366-018-0657-8
47. Sahmani S, Khandan A (2018) Size dependency in nonlinear instability of smart magneto-electro-elastic cylindrical composite nanopanels based upon nonlocal strain gradient elasticity. Microsyst Technol. https://doi.org/10.1007/s00542-018-4072-2
48. Sahmani S, Aghdam MM (2018) Nonlocal electrothermomechanical instability of temperature-dependent FGM nanopanels with piezoelectric facesheets. Iran J Sci Technol Trans Mech Eng. https://doi.org/10.1007/s40997-018-0180-y

49. Babu B, Patel BP (2019) Analytical solution for strain gradient elastic Kirchhoff rectangular plates under transverse static loading. Eur J Mech A Solids 73:101–111
50. Sarafraz A, Sahmani S, Aghdam MM (2019) Nonlinear secondary resonance of nanobeams under subharmonic and superharmonic excitations including surface free energy effects. Appl Math Model 66:195–226
51. Gao Y, An L (2010) A nonlocal elastic anisotropic shell model for microtubule buckling behaviors in cytoplasm. Physica E 42:2406–2415
52. Taj M, Zhang JQ (2012) Analysis of vibrational behaviors of microtubules embedded within elastic medium by Pasternak model. Biochem Biophys Res Commun 424:89–93
53. Baninajjaryan A, Tadi Beni Y (2015) Theoretical study of the effect of shear deformable shell model, elastic foundation and size dependency on the vibration of protein microtubule. J Theor Biol 382:111–121
54. Civalek B, Demir C (2016) A simple mathematical model of microtubules surrounded by an elastic matrix by nonlocal finite element method. Appl Math Comput 289:335–352
55. Deng J, Liu Y, Zhang Z, Liu W (2017) Size-dependent vibration and stability of multi-span viscoelastic functionally graded material nanopipes conveying fluid using a hybrid method. Compos Struct 179:590–600
56. Sahmani S, Aghdam MM (2017) Size-dependent axial instability of microtubules surrounded by cytoplasm of a living cell based on nonlocal strain gradient elasticity theory. J Theor Biol 422:59–71
57. Sahmani S, Aghdam MM (2017) Nonlinear instability of hydrostatic pressurized microtubules surrounded by cytoplasm of a living cell including nonlocality and strain gradient microsize dependency. Acta Mech 229:403–420
58. Sahmani S, Aghdam MM (2017) Nonlinear vibrations of pre- and post-buckled lipid supramolecular micro/nano-tubules via nonlocal strain gradient elasticity theory. J Biomech 65:49–60
59. Lim CW, Zhang G, Reddy JN (2015) A higher-order nonlocal elasticity and strain gradient theory and its applications in wave propagation. J Mech Phys Solids 78:298–313
60. Li L, Hu Y (2015) Buckling analysis of size-dependent nonlinear beams based on a nonlocal strain gradient theory. Int J Eng Sci 97:84–94
61. Li L, Hu Y (2016) Wave propagation in fluid-conveying viscoelastic carbon nanotubes based on nonlocal strain gradient theory. Comput Mater Sci 112:282–288
62. Yang WD, Yang FP, Wang X (2016) Coupling influences of nonlocal stress and strain gradients on dynamic pull-in of functionally graded nanotubes reinforced nano-actuator with damping effects. Sens Actuators, A 248:10–21
63. Simsek M (2016) Nonlinear free vibration of a functionally graded nanobeam using nonlocal strain gradient theory and a novel Hamiltonian approach. Int J Eng Sci 105:10–21
64. Farajpour A, Haeri Yazdi MR, Rastgoo A, Mohammadi M (2016) A higher-order nonlocal strain gradient plate model for buckling of orthotropic nanoplates in thermal environment. Acta Mech 227:1849–1867
65. Tang Y, Liu Y, Zhao D (2017) Wave dispersion in viscoelastic single walled carbon nanotubes based on the nonlocal strain gradient Timoshenko beam model. Physica E 87:301–307
66. Sahmani S, Aghdam MM (2018) Nonlocal strain gradient beam model for postbuckling and associated vibrational response of lipid supramolecular protein micro/nano-tubules. Math Biosci 295:24–35
67. Li X, Li L, Hu Y, Ding Z, Deng W (2017) Bending, buckling and vibration of axially functionally graded beams based on nonlocal strain gradient theory. Compos Struct 165:250–265
68. Lu L, Guo X, Zhao J (2017) Size-dependent vibration analysis of nanobeams based on the nonlocal strain gradient theory. Int J Eng Sci 116:12–24
69. Sahmani S, Aghdam MM (2017) Nonlinear instability of axially loaded functionally graded multilayer graphene platelet-reinforced nanoshells based on nonlocal strain gradient elasticity theory. Int J Mech Sci 131:95–106
70. Sahmani S, Aghdam MM (2017) A nonlocal strain gradient hyperbolic shear deformable shell model for radial postbuckling analysis of functionally graded multilayer GPLRC nanoshells. Compos Struct 178:97–109
71. Sahmani S, Aghdam MM, Rabczuk T (2018) Nonlinear bending of functionally graded porous micro/nano-beams reinforced with graphene platelets based upon nonlocal strain gradient theory. Compos Struct 186:68–78
72. Sahmani S, Aghdam MM, Rabczuk T (2018) A unified nonlocal strain gradient plate model for nonlinear axial instability of functionally graded porous micro/nano-plates reinforced with graphene platelets. Mater Res Express 5:045048
73. Sahmani S, Aghdam MM, Rabczuk T (2018) Nonlocal strain gradient plate model for nonlinear large-amplitude vibrations of functionally graded porous micro/nano-plates reinforced with GPLs. Compos Struct 198:51–62
74. Zhen Y-X, Wen S-L, Tang Y (2019) Free vibration analysis of viscoelastic nanotubes under longitudinal magnetic field based on nonlocal strain gradient Timoshenko beam model. Physica E 105:116–124
75. Sawant MK, Dahake AG (2014) A new hyperbolic shear deformation theory for analysis of thick beam. Int J Innov Res Sci Eng Technol 3:9636–9643
76. Faghih Shojaei M, Ansari R, Mohammadi V, Rouhi H (2014) Nonlinear forced vibration analysis of postbuckled beams. Arch Appl Mech 84:421–440
77. Ansari R, Mohammadi V, Faghih Shojaei M, Gholami R, Sahmani S (2014) On the forced vibration analysis of Timoshenko nanobeams based on the surface stress elasticity theory. Compos B Eng 60:158–166
78. Sahmani S, Bahrami M, Aghdam MM, Ansari R (2014) Surface effects on the nonlinear forced vibration response of third-order shear deformable nanobeams. Compos Struct 118:149–158
79. Keller BH (1977) Numerical solution of bifurcation and nonlinear eigenvalue problems, applications of bifurcation theory. University of Wisconsin, Madison, New York
80. de Pablo PJ, Schaap IAT, Mackintosh FC, Schmidt CF (2003) Deformation and collapse of microtubules on the nanometer scale. Phys Rev Lett 91:098101